
COMBINING MULTI-FIDELITY MODELLING AND ASYNCHRONOUS BATCH BAYESIAN OPTIMIZATION

A PREPRINT

Jose Pablo Folch ^{*}
 Imperial College London
 London, UK
 jose.folch16@imperial.ac.uk

Robert M Lee
 BASF SE
 Ludwigshafen, Germany
 robert-matthew.lee@bASF.com

Behrang Shafei
 BASF SE
 Ludwigshafen, Germany
 behrang.shafei@bASF.com

David Walz
 BASF SE
 Ludwigshafen, Germany
 david-simon.walz@bASF.com

Calvin Tsay
 Imperial College London
 London, UK
 c.tsay@imperial.ac.uk

Mark van der Wilk
 Imperial College London
 London, UK
 m.vdwilk@imperial.ac.uk

Ruth Misener
 Imperial College London
 London, UK
 r.misener@imperial.ac.uk

ABSTRACT

Bayesian Optimization is a useful tool for experiment design. Unfortunately, the classical, sequential setting of Bayesian Optimization does not translate well into laboratory experiments, for instance battery design, where measurements may come from different sources and their evaluations may require significant waiting times. Multi-fidelity Bayesian Optimization addresses the setting with measurements from different sources. Asynchronous batch Bayesian Optimization provides a framework to select new experiments before the results of the prior experiments are revealed. This paper proposes an algorithm combining multi-fidelity and asynchronous batch methods. We empirically study the algorithm behavior, and show it can outperform single-fidelity batch methods and multi-fidelity sequential methods. As an application, we consider designing electrode materials for optimal performance in pouch cells using experiments with coin cells to approximate battery performance.

Keywords Bayesian Optimization · Machine Learning · Batch Optimization · Asynchronous · Multi-fidelity

1 Introduction

The optimal design of many engineering processes can be subject to expensive and time-consuming experimentation. For efficiency, we seek to avoid wasting valuable resources in testing sub-optimal designs. One way to achieve this is by obtaining cheaper approximations of the desired system, which allow us to quickly explore new regimes and avoid areas that are clearly sub-optimal. As an example, consider the case diagrammed in Figure 1 from battery materials research with the goal of designing electrode materials for optimal performance in pouch cells. We can use experiments with cheaper coin cells and shorter test procedures to approximate the behaviour of the material in longer stability tests in pouch cells, which is in turn closer to the expected performance in electric car applications [Chen et al., 2019, Dörfler et al., 2020, Liu et al., 2021]. Similarly, design goals regarding battery life such as discharge capacity retention can be approximated using an early prediction model on the first few charge cycles rather than running aging and stability tests to completion [Attia et al., 2020].

^{*}Corresponding author.

Furthermore, in most applications it is infeasible to wait for a single experiment to end before planning new ones, due to the long waiting times for the experiments to finish (from a few weeks to months). This means that in practice experiments will be carried out in batch or in parallel. However, owing to the introduction of cheaper approximations and variations in material degradation rates, experiments may not finish simultaneously. For example, if our experimental batch consists of a mixture of cells tested with slower and accelerated test procedures, some results will become available in a few weeks, whereas others can take *months*. In the meantime, we do not want to leave resources idle while we wait for all experiments to be finished. Therefore, we must select new experiments before receiving the full results from those still in progress. This inspires the question: *How can we automatically and continuously design new experiments when the prior experimental data returns on different (and uncertain) time-frames and the type of measurements may vary?*

Design of experiments is a well-studied area, with applications ranging from parameter estimation [Asprey and Macchietto, 2000, Box and Lucas, 1959, Waldron et al., 2019] and model selection [Hunter and Reiner, 1965, Tsay et al., 2017] in chemistry, to psychology survey design [Vincent, 2016, Foster et al., 2021]. Many of these works assume an underlying model which we want to learn efficiently. See Franceschini and Macchietto [2008] for a comprehensive overview of model-based design of experiments and Wang and Dowling [2022a] for computational considerations. However, our particular focus lies in designing experiments for optimizing black box functions [Bajaj et al., 2021]. Specifically, these are complex and expensive-to-evaluate functions from which we do not receive gradient information. We can select a sequence of function inputs, from which we observe a sequence of outputs.

Bayesian Optimization (BO) [Jones et al., 1998, Shahriari et al., 2016] optimizes black-box functions using probabilistic surrogate models, which manage the trade-off between exploiting promising experiments and exploring unseen design space [Bhosekar and Ierapetritou, 2018]. Such methods have been successfully applied in the area of chemical engineering [Thebelt et al., 2022a].

This paper focuses on recent advances in multi-fidelity BO [Kandasamy et al., 2016a, Takeno et al., 2020] and Batch BO [González et al., 2016, Alvi et al., 2019, Kandasamy et al., 2018, Snoek et al., 2012]. Multi-fidelity BO uses cheap approximations of the objective function to speed up the optimization process. Batch BO selects multiple experiments at the same time. We explore the close relationship between both research areas, provide an overview of the current state-of-the-art, and introduce a general algorithm that allows practitioners to *simultaneously* take advantage of multi-fidelity and batching while using any acquisition function of their choice, significantly speeding up Bayesian Optimization procedures. We show the usefulness of the method by applying it to synthetic benchmarks, a high-dimensional example, and real life-experiments relating to coin and pouch cell batteries tested with different measurement procedures.

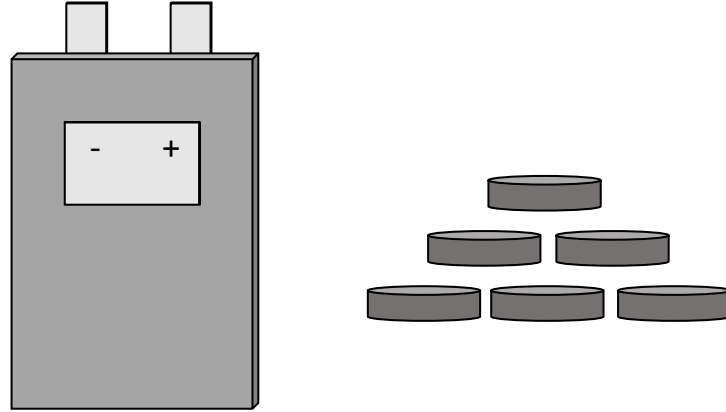


Figure 1: Motivating example. On the left is pouch-cell battery and on the right are coin cell batteries [Chen et al., 2019, Dörfler et al., 2020, Liu et al., 2021]. Using coin cells, which are cheaper and faster to make than pouch batteries, we can approximate the behaviour of our target. Usually these experiments are carried out in large batches.

2 Related Work

Bayesian Optimization (BO) has been well researched in the domain of tuning the hyper-parameters of computationally expensive machine learning models [Bergstra et al., 2011, Li et al., 2017]. However, to be efficiently applicable to chemical engineering there is a need to adapt and improve such methods [Amaran et al., 2016, Thebelt et al., 2022a, Wang and Dowling, 2022b]. For example, Folch et al. [2022] considers the physical cost of changing from one

experimental set-up to another and Thebelt et al. [2021, 2022b,c] allow input constraints in addition to the black-box functions. The related area of *grey-box optimization* seeks to solve optimal decision-making problems incorporating both black-box, data-driven models and mechanistic, equation-based models [Cozad et al., 2014, Boukouvala and Floudas, 2017, Olofsson et al., 2018, Park et al., 2018, Paulson and Lu, 2022, Kudva et al., 2022].

The multi-fidelity setting has been gaining attention in machine learning research recently. Multi-fidelity BO uses cheap approximations of the objective function to explore the input space more efficiently, and saves full evaluations for more promising areas. Different approaches for modelling the multi-fidelity using Gaussian Processes (GPs) have been developed [Kennedy and O'Hagan, 2000, Gratiet, 2013, Cutajar et al., 2019]. In terms of Bayesian Optimization, there has been research from the basic k-armed bandit problem [Kandasamy et al., 2016b] to more general non-GP based methods [Sen et al., 2018]. This paper addresses the setting and method introduced in Kandasamy et al. [2016a], where we use an independent GP to model each fidelity. Each fidelity is linked by a bias assumption which allows the transfer of information by taking the tightest of many upper confidence bounds. As a more efficient alternative, we will also explore multi-task Gaussian Processes [Journel and Huijbregts, 1976, Goovaerts et al., 1997, Alvarez et al., 2012].

Multi-fidelity shares a close relationship with transfer learning [Zhuang et al., 2021, Pan and Yang, 2009], which has seen many successful engineering applications Li et al. [2020], Li and Rangarajan [2022], Jia et al. [2020], Rogers et al. [2022]. In transfer learning, we seek to get improved performance in a target task by using data from similar tasks that have been carried out in the past. Multi-fidelity optimization can be thought of as transfer learning, where we can actively *choose* to increase the data of auxiliary data-sets.

Asynchronous BO chooses queries while waiting for delayed observations. Kandasamy et al. [2018] proposed a method based on Thompson Sampling, using the method's natural randomness to ensure variety in experiments. Ginsbourger et al. [2011] introduce a variant of Expected Improvement, which seeks to integrate out ongoing queries, and uses Monte Carlo methods to estimate the acquisition function. Snoek et al. [2012] introduces a more general version of this idea that 'fantasizes' delayed observations. González et al. [2016] and Alvi et al. [2019] propose mimicking sequential BO by *penalizing* the acquisition function at points where we are asynchronously running experiments.

An example where multi-fidelity approximations are being applied is on the area of molecule design and synthesis [Alshehri et al., 2020], where we can use cheap computer approximations to search the space of molecules, and then choose which real experiments to carry out based on the best performing simulations [Coley, 2021]. Coley et al. [2019] use computer simulations to determine feasibility in synthesizing organic compounds, and then use a robotic arm that carries out experiments in batch. This is could be seen as having a multi-fidelity step followed by a batching step, however, the methods are carried out separately.

Recently, Li et al. [2021] combined batch and multi-fidelity methods using Bayesian Neural Networks (BNNs). This work focuses on simpler, more robust and computationally feasible methods that work directly on the asynchronous setting. Takeno et al. [2020] propose a multi-fidelity BO algorithm based on max-entropy search [Wang and Jegelka, 2017], specializing in asynchronous batching, we take inspiration from this work and generalize it to help avoid the computational complexities of the method, and possible pitfalls from being constrained to a single acquisition function. More recently, GIBBON [Moss et al., 2021] was proposed as a general-purpose extension of max-entropy search, by using cheap-approximations to the information gain.

3 Multi-fidelity Modelling

Optimal experiment design relies on surrogate models to convey information about our knowledge of the search space. The surrogate model represents our *belief* of how the underlying black-box function looks like. Selecting new experiments near our surrogate's optimum is known as *exploiting*, which is when we choose new experiments close to the best experiments we have observed so far. It is also important for the model to provide some measure of *uncertainty* [Hüllen et al., 2020], which we can leverage to *explore* the search space. Uncertainty should be high in areas where we do not have any data, and low where we have a lot of data.

We assume we are trying to model a function f . However, we have access to M auxiliary functions, $f^{(m)}$, which approximate f for $m = 1, \dots, M$. Each function will have a data-set, $D^{(m)} = \{(x_i^{(m)}, y_i^{(m)})\}_{i=1}^{N_m}$ consisting of noisy observations of each function:

$$y_i^{(m)} = f^{(m)}(x_i^{(m)}) + \eta^{(m)}\epsilon_i, \quad (1)$$

where $\epsilon_i \sim \mathcal{N}(0, 1)$. We want a model that will use information from all data-sets to have a more accurate model of the objective $f = f^{(M)}$. For example, in the battery example, we have access to $M = 2$ types of data – the cheaper coin cell battery data, and the target pouch cell battery data. We want to use both types of data together, to obtain a more accurate model for pouch cell batteries.

This paper uses Gaussian Process (GP) surrogate models [Rasmussen and Williams, 2005], which are very flexible and have well calibrated uncertainty estimates. A GP is a stochastic processes defined by a mean function, $\mu(\cdot) : \mathcal{X} \rightarrow \mathbb{R}$, and a positive-definite co-variance function $k(\cdot, \cdot) : \mathcal{X} \times \mathcal{X} \rightarrow \mathbb{R}$. In particular, given a data-set $D = \{(x_i, y_i)\}_{i=1}^N$ if we select a GP prior on $f \sim \mathcal{GP}(\mu_0, k_0)$, then we can consider the Gaussian likelihood:

$$y | f, \eta^2 \sim \mathcal{N}(f, \eta^2 I).$$

This allows us to explicitly compute the posterior of f , which is also a GP. More precisely, $f | D_t \sim \mathcal{GP}(\mu_t, k_t^2)$:

$$\begin{aligned} \mu_t(x) &= \mu_0(x) + k_0(x)^T (K + \eta^2 I)^{-1} (y - m) \\ k_t^2(x, x') &= k_0(x, x') - k(x)^T (K + \eta^2 I)^{-1} k(x'), \end{aligned}$$

where $m_i = \mu_0(x_i)$, $k(x)_i = k_0(x, x_i)$, $K(x)_{i,j} = k(x_i, x_j)$. As we will see, we can use this posterior to build an acquisition function to select the next experiment.

3.1 Independent Gaussian Processes

The first model we consider is the simplest. We fit an independent GP to each model. That is, we assume the prior:

$$f^{(m)} \sim \mathcal{GP}(\mu_0^{(m)}, k_0^{(m)}), \quad (2)$$

and obtain the posterior independently, that is, for each fidelity $m = 1, \dots, M$, the posterior is obtained by only conditioning on each fidelities data-set: $f^{(m)} | \cup_{m'=1}^M D^{(m')} = f^{(m)} | D^{(m)}$. There are two main benefits to this approach: (a) This is the simplest and computationally cheapest out of all exact inference GP methods. (b) It is the easiest on which to intuitively impose prior knowledge and information. However, the main drawback is significant: there is no transfer of information between the fidelities, so we will be forced to make simplifying assumptions relating to hierarchy and bias at the time of optimization.

3.2 Multi-task Gaussian Processes

A more complete approach seeks to *jointly* model all fidelities. One effective and popular approach is to use a multi-task Gaussian Process [Alvarez et al., 2012]. This approach models each fidelity as an output of a Multi-output Gaussian Processes (MOGP). Instead of having a scalar-valued mean function, we have a M -dimensional vector valued function, $\mu : \mathcal{X} \rightarrow \mathbb{R}^M$ and a $M \times M$ -dimensional matrix valued co-variance function $K : \mathcal{X} \times \mathcal{X} \rightarrow \mathbb{R}^{M \times M}$, where the (m, m') th entry of $K(x, x')$ corresponds to the covariance of $f^{(m)}(x)$ and $f^{(m')}(x')$.

We focus on separable kernels and on the Linear Model of Coregionalization [Journel and Huijbregts, 1976, Goovaerts et al., 1997]. A *separable kernel* is where the input-dependence and the fidelity dependence can be separated into a product:

$$K(x, x')_{m,m'} = k^{(I)}(x, x') k^{(F)}(m, m') \quad (3)$$

where $k^{(I)}$ and $k^{(F)}$ are scalar kernels corresponding to the inputs and fidelities correspondingly. In matrix notation this can be written as:

$$K(x, x') = k_I(x, x') \mathcal{B} \quad (4)$$

where k_I is now a matrix-valued kernel, and \mathcal{B} is a matrix weighting the task-dependencies. The sum of kernels is also a valid kernel, therefore we can create more flexible models by considering the *sum* of W separable kernels:

$$K(x, x') = \sum_{w=1}^W k_w^{(I)}(x, x') \mathcal{B}_w \quad (5)$$

This allows us to have different types of kernels in the sum, or kernels with different hyper-parameters within the same model. The class of MOGP models with kernels given as (5) is known as the Linear Model of Coregionalization (LMC). Special cases of the model include the Intrinsic Coregionalization Model [Goovaerts et al., 1997] (where all kernels k_w are the same) and the Semi-parametric Latent Factor Model [Teh et al., 2005].

The main benefit of using these models is that the task-dependency is learnt from the data! We learn to transfer information from the lower-fidelities to the target fidelity. The drawbacks against independent models are (i) higher computational expense when doing exact inference and (ii) the kernel hyper-parameters become difficult to set manually.

3.3 Further Extensions

This paper limits itself to the methods mentioned above. However, we mention a few more complicated models that could be used when needed. The LMC is limited because it assumes that the co-variance function is a linear combination of separable kernels. A more general model allows for non-separable kernels by considering processes convolutions [Ver Hoef and Barry, 1998, Higdon, 2002, van der Wilk et al., 2017]. Deep Gaussian Processes [Damianou and Lawrence, 2013] have also been used to model multi-fidelity systems, where each layer represents a fidelity [Cutajar et al., 2019]. Li et al. [2021] use Bayesian Neural Networks [MacKay, 1992, Neal, 2012] rather than Gaussian Processes, thereby allowing for learning of complex non-linearities while still providing uncertainty estimates. However, such models are notoriously difficult to train [Izmailov et al., 2021]. We were interested in applying Bayesian Neural Networks models, but, we were unable to consistently obtain good inference so we discarded them from our analysis.

4 Bayesian Optimization

Bayesian Optimization (BO) considers the problem of finding:

$$x_* = \arg \max_{x \in \mathcal{X}} f(x) \quad (6)$$

where f is a black box function, and \mathcal{X} is some d -dimensional input space. The function can be evaluated at any arbitrary point, $x \in \mathcal{X}$, and this leads to noise corrupted observations of the form:

$$y = f(x) + \epsilon$$

where ϵ is zero-mean noise. BO places a surrogate model on f and uses this model to generate an acquisition function, $\alpha : \mathcal{X} \rightarrow \mathbb{R}$. This function is used to select the sequence of inputs, i.e., to design subsequent experiments. Given a data set $D_t = \{(x_i, y_i)\}_{i=1}^t$, we select a new point, x_{t+1} , by optimizing the acquisition function:

$$x_{t+1} = \arg \max_{x \in \mathcal{X}} \alpha(x; D_t)$$

4.1 Multi-fidelity Bayesian Optimization

One of the main ideas in BO is managing the trade-off between exploration and exploitation. The algorithm has to decide between experimenting in promising areas where it has observed high values of f , against choosing to experiment in areas where there is little information. If there is too much exploration, the algorithm will take too long to find the optimum. However, if there is too much exploitation, the algorithm might settle in a sub-optimal area.

More concretely, at time t , we assume that we can *choose* an input-fidelity pair, (x_t, m) , from which we obtain a possibly noise observation, $y_t^{(m)}$ of the m th fidelity function, $f^{(m)}$, as in Equation (1).

And the target of the optimization is to maximize the function at the highest fidelity $f^{(M)}$. We further assume that each fidelity will have a known cost $C^{(m)}$, which is lower than the cost at the highest fidelity. For the purposes of this paper, we will assume the cost refers to a measure of *time*. However, it could represent financial costs, man-power, etc... We clarify that we assume the costs are scalar-values known *a priori*. While it would be useful to consider a trade-off between different types of costs, this is left to future work.

Multi-fidelity methods allow us to use cheap approximations to explore while saving the expensive evaluations for a separate exploitation phase of the algorithm. All multi-fidelity methods follow the same pattern: at first they will query the lower fidelities and as the optimization loop progresses we begin to query the target fidelity.

4.1.1 Multi-fidelity Upper Confidence Bound

Kandasamy et al. [2016a] propose one of the most intuitive and simplest methods. They show that by making the right assumptions, you are able to use independent Gaussian Processes for each fidelity and still transfer information effectively by using Upper Confidence Bounds (UCB). The UCB acquisition function, for a Gaussian Process posterior with mean function, $\mu_t(\cdot)$, and variance function $\sigma_t^2(x)$ is given by:

$$\alpha_{UCB}(x; \beta_t, D_t) = \mu_t(x) + \beta_t^{1/2} \sigma_t(x) \quad (7)$$

Here, $\beta_t > 0$ is a hyper-parameter that balances how much we value the uncertainty when deciding which point to choose next. A large value represents being optimistic about areas where we are uncertain and will naturally lead to more exploration and reduced exploitation. In practice, β_t is usually chosen as an increasing logarithmic function which allows us to have theoretical guarantees.

Assume that there are M different fidelities, and we are interested in optimizing the highest fidelity, $f^{(M)} := f$. The key assumption is that there is a decreasing *known* maximum bias among the fidelities, such that:

$$\|f^{(m)} - f\|_{\infty} := \max_{x \in \mathcal{X}} |f^{(m)}(x) - f(x)| \leq \zeta_{MAX}^{(m)} \quad (8)$$

For $\zeta_{MAX}^{(1)} \geq \zeta_{MAX}^{(2)} \geq \dots \geq \zeta_{MAX}^{(M)} = 0$.

To combine information from multiple fidelities, we begin by fitting an independent GP to the data for each fidelity. That is, for each fidelity m , there is a data-set $D_t^{(m)}$ of experiments, so that $f^{(m)} | D_t^{(m)} \sim \mathcal{GP}(\mu_t^{(m)}, k_t^{(m)})$. Then the upper confidence bound is defined as:

$$\alpha^{(m)}(x; D_t^{(m)}) = \mu_t^{(m)}(x) + \beta_t^{1/2} \sigma_t^{(m)}(x) + \zeta_{MAX}^{(m)}$$

where $(\sigma_t^{(m)})^2(x) = (k_t^{(m)})^2(x)$. By adding the bias, each of these functions represents an upper bound on the *objective* fidelity. Therefore we can build a narrow bound by considering the minimum of all the upper confidence bounds at each possible input x . With this idea in mind, the acquisition function is then defined as:

$$\alpha(x; D_t) = \min_{m \in \{1, \dots, M\}} \alpha^{(m)}(x; D_t^{(m)}) \quad (9)$$

Figure 2 gives a graphical example of building this acquisition function.

The next experiment is chosen by maximizing the acquisition function given by (9). However, the choice of a fidelity level still remains. Consider the standard deviation of the surrogate model for fidelity m at input x_{t+1} , $\sigma_t^{(m)}(x_{t+1})$. If this quantity is high, it means there remains a lot of information to learn about fidelity m at our specific input. If this quantity is low, it means we cannot learn much from experimenting at this fidelity.

Therefore we define a set of threshold levels $\{\gamma^{(m)}\}_{m=1}^M$. If the posterior variance is smaller than the corresponding threshold, we cannot learn much about the objective function by sampling at this lower fidelity so it is better to choose a higher fidelity. To try to minimize the cost of evaluation, we choose the lowest fidelity that contains enough information according to the thresholds. More precisely, the choice is given by:

$$m_{t+1} = \arg \min_{m \in \{0, \dots, M\}} \{m : \beta_t^{1/2} \sigma_t^{(m)} > \gamma^{(m)} \text{ or } m = M\} \quad (10)$$

We note that this idea for choosing the fidelity is not restricted to upper-confidence bound acquisition functions. In fact, we can use *any* acquisition function and then choose the fidelity with rule defined by equation (10). We shall see that combining this rule with LMCs means we can drop the bias assumption and obtain better results than using independent GPs.

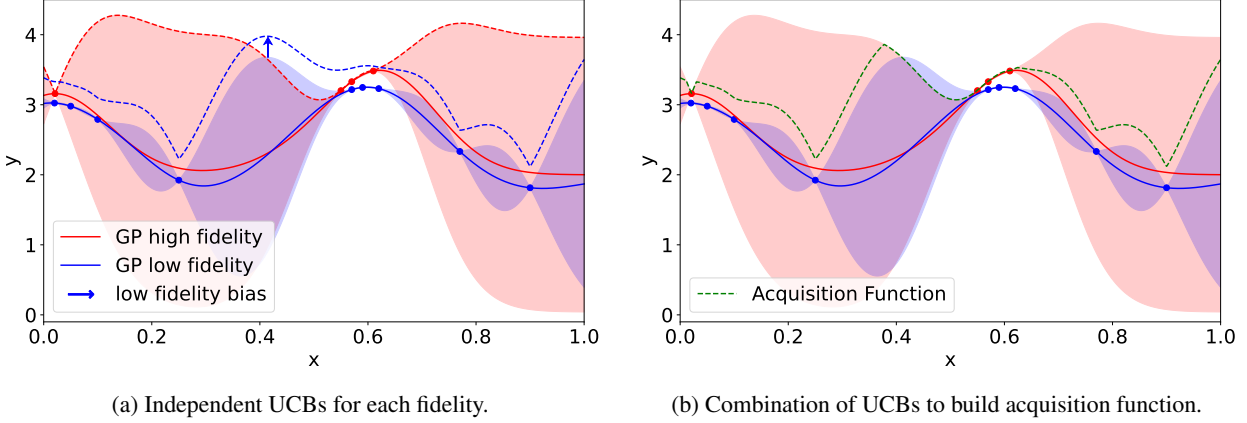


Figure 2: Building an multi-fidelity UCB, in the case where $M = 2$. The dotted lines represent upper confidence bounds based on bias and variances. In the first figure we can see the bounds for each independent fidelity, in the second figure both bounds are combined to obtain the final acquisition function.

4.1.2 Multi-fidelity Max Entropy Search

Information-based methods have become increasingly popular in Bayesian Optimization due to their strong theoretical backing. Entropy search [Villemonteix et al., 2009, Hennig and Schuler, 2012, Hernández-Lobato et al., 2014] tries to maximize the information gain about the optimum input, x_* . Unfortunately, this means estimating an expensive d -dimensional integral using Monte Carlo approximations. Max-value Entropy Search [Wang and Jegelka, 2017] instead focuses on maximizing the information gain about the maximum value of the function, $f_* = f(x_*)$:

$$\alpha_t(x) = I((x, f(x); f_*|D_t) = H(p(y|D_t, x)) - \mathbb{E}_{f_*|D_t} [p(y|D_t, x, f_*)] \quad (11)$$

Which means the integral estimation is reduced from d -dimensional to 1-dimensional. The expectation is estimated using Monte Carlo methods since we are able to sample from the distribution $p(f_*|D_t)$ via Thompson Sampling or an approximation via the Gumbel distribution. More recently, Tu et al. [2022] and Hvarfner et al. [2022] jointly consider the joint information gain of both the maximum value, and the optimum input.

A multi-fidelity extension of Max-value Entropy Search was introduced by Takeno et al. [2020]. We easily extend to the multi-fidelity setting by considering a joint model, such as the LMC and then maximizing the cost-weighted information gain:

$$\alpha_t(x, m|D_t) = \frac{I(x, f^{(m)}(x); f_*|D_t)}{C^{(m)}} = \frac{I(x, f^{(m)}(x); f_*|D_t)}{C^{(m)}} \quad (12)$$

The biggest strength of this method, when compared to multi-fidelity upper confidence bound, is that we are not longer using independent GPs as a model. As such, we can *learn* the relationship between the functions and there is no need to make assumptions about the maximum bias. There are also no hyper-parameters in the acquisition function.

4.2 Asynchronous Batch Bayesian Optimization

So far we have focused on sequential Bayesian Optimization. However, in some battery experiments, we cannot wait for the experiment results to return before choosing the next point, we must do this in batch. It is also important to note that we expect different fidelity levels to have a considerably different evaluation time. This can be a problem as most batch methods focus on the synchronous setting. That is, you select a batch, wait for all evaluations to return, and then select another. Large time discrepancies in the evaluation times pose a problem, as there are a lot of resources that will be left idle while longer evaluations finish. As such, we are more interested in the less-studied asynchronous setting.

Throughout this section, assume we are in the normal setting of Bayesian Optimization, however, further assume that at time t we are evaluating a batch of points $\mathcal{Q}_t = \{x_{t,q}\}_{q=1}^Q$ whose observations, $f_{\mathcal{Q}}$, we still do not know. We are then interested in choosing the next experiment while taking \mathcal{Q} into account, so that the acquisition function depends on the pending evaluations:

$$x_{t+1} = \arg \max_{x \in \mathcal{X}} \alpha_t(x|D_t, \mathcal{Q}_t) \quad (13)$$

4.2.1 Thompson Sampling

Thompson Sampling is a common technique in Bayesian decision making that uses samples from the posterior distribution to guide actions. Kandasamy et al. [2018] show it can be used effectively for Asynchronous Batch BO. A sample is selected by maximizing a sample from the posterior GP:

$$\begin{aligned} f_{\text{sample}} &\sim \mathcal{GP}(\mu_t, \kappa_t|D_t) \\ x_{t+1} &= \arg \max_{x \in \mathcal{X}} f_{\text{sample}}(x) \end{aligned} \quad (14)$$

Note that the new point selected is *independent* of \mathcal{Q} , however, the randomness in the sampling is enough to ensure diversity in the batch. Due to the independence, it works well in the asynchronous batch setting, and large batches can be created cheaply.

4.2.2 Parallel Querying Through Fantasies

Snoek et al. [2012] allow for the asynchronous batching of any acquisition function. This can be achieved by creating multiple ‘fantasies’ at every point in \mathcal{Q} , and then using them to marginalize out the pending observations, $f_{\mathcal{Q}}$:

$$\begin{aligned} \alpha_t(x|D_t, \mathcal{Q}_t) &= \int \alpha(x|D_t, f_{\mathcal{Q}}, \mathcal{Q}_t) p(f_{\mathcal{Q}}|D_t) df_{\mathcal{Q}} \\ &\approx \frac{1}{S} \sum_{s=1}^S \alpha_t(x|D_t \cup \{\tilde{f}_{\mathcal{Q}}^{(s)}, \mathcal{Q}_t\}) \end{aligned} \quad (15)$$

where $\tilde{f}_{\mathcal{Q}}^{(s)}$ are sample drawn from the normal distribution $f_{\mathcal{Q}}|D_t$, and S is the number of samples. Note that we are trying to estimate a Q -dimensional integral, so the larger the number of fantasies, the better the approximation but the computational expense increases. One consideration though, is that we *do not* need to fully re-train the Gaussian Process for every fantasy. This is because the variance of the posterior only depends on the input locations, \mathcal{Q} , which are the same for every fantasy. Instead, we only need to re-train the mean of the process which is much cheaper.

In the case of Max-value Entropy Search, Takeno et al. [2020] show that using fantasies, the Q -dimensional integral can be written as a 2-dimensional integral which means we do not need as many fantasies to get good approximations.

4.2.3 Local Penalization

Local penalization is a batch Bayesian Optimization introduced by González et al. [2016], and which was then easily extended to the asynchronous setting by Alvi et al. [2019].

The method relies on trying to mimic the sequential setting, where after receiving experimental information about a particular input we usually expect the acquisition function to decrease in the neighbourhood surrounding this point. More precisely, assume we wish to select a new point x_t , then we can mimic the sequential setting by defining the new acquisition function, $\tilde{\alpha}$, as:

$$\tilde{\alpha}(x; D_t, \mathcal{Q}) = g(\alpha(x; D_t)) \prod_{x_{t,q} \in \mathcal{Q}} \psi(x_{t,q}) \quad (16)$$

where $\psi(x)$ is a function that penalizes the region around x , and $g(\cdot)$ is a differentiable transformation that makes sure the acquisition function is positive. We use $g(z) = z$ for positive acquisition functions, and the soft-max transformation otherwise, $g(z) = \log(1 + e^z)$. The question then becomes, how do we choose such penalizers? To do this, we begin by assuming that the function satisfies the Lipschitz condition. That is, if \mathcal{X} is compact, then:

$$|f(x_1) - f(x_2)| \leq L \|x_1 - x_2\| \quad \forall x_1, x_2 \in \mathcal{X}$$

where $L \in \mathbb{R}^+$, and $\|\cdot\|$ is the L^2 norm in \mathbb{R}^d . We now consider the ball, around arbitrary $x_j \in \mathcal{X}$:

$$B_{r_j}(x_j) = \{x \in \mathcal{X} : \|x_j - x\| \leq r_j\}$$

where the radius r_j is given by:

$$r_j = \frac{f(x_*) - f(x_j)}{L} =: r(x_j)$$

The radius is chosen because, if the Lipschitz assumption holds, then x_* cannot lie inside this ball. Note that due to f being modeled by a GP, then this radius is a random quantity. González et al. [2016] then define the local penaliser as follows:

$$\psi(x; x_j) = 1 - p(x \in B_{r_j}(x_j))$$

That is, we choose the local penalizer to be the probability that x does not lie inside $B_{r_j}(x_j)$. However, Alvi et al. [2019] argue that this penalizer may lead to redundantly sampling the same points. Instead they propose the penalizer:

$$\psi(x; x_j) = \min \left\{ \frac{\|x - x_j\|}{\mathbb{E}(r_j) + \sigma_t(x_j)/L}, 1 \right\} \quad (17)$$

Figure 3 shows an example of how the penalization can be used to alter the acquisition function to choose a new experiment.

4.3 Relationship between multi-fidelity and asynchronous batch methods

Ultimately the goal of using multi-fidelity and batch methods is to speed up the optimization by using extra tools available to us. Multi-fidelity methods use cheap and fast to obtain approximations to the objective, while batching takes advantage of running experiments in parallel. Therefore it is natural to want to use both methods at the same time to obtain even more speed gains in optimization procedures.

However, we emphasise that we cannot fully use both tools simultaneously without asynchronicity arising. Indeed, by definition, lower fidelity approximations are meant to be cheaper and faster to obtain. This means if we select a batch of evaluations, those of lower fidelities will finish earlier than high fidelity evaluations. Without any asynchronicity we must wait for all experiments to finish before deciding the next batch, making the method inefficient.

There can also be strong relationships between fidelity and *batch size*. Indeed, it might be the case that many low fidelity experiments can easily be done in parallel, but due to having to use more resources, for high fidelities we can only parallelize a few. An example of this could be as simple as trying out cake recipes. A full fidelity observation

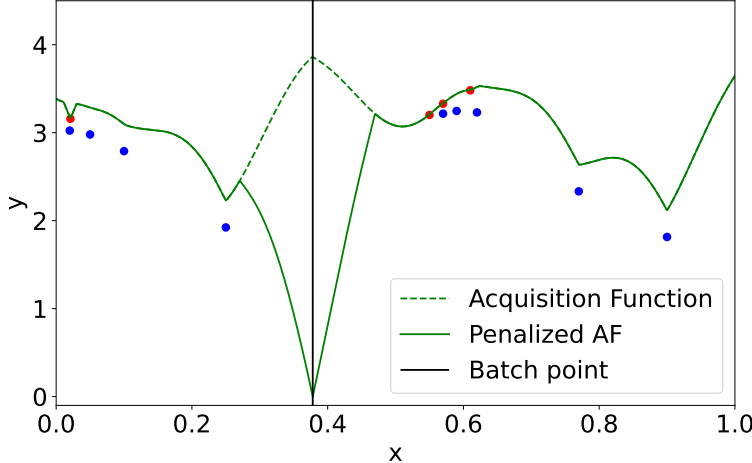


Figure 3: An example of the local penalization process. We selected $x = 0.378$ as a point to evaluate. The acquisition function is then penalized as shown above until we obtain a new observation. This allows us to select new queries without receiving an observation, as the penalized acquisition function is guaranteed to have a different maximum. The blue and red dots represent low and high fidelity observations, respectively.

would be baking a cake in the oven; while low fidelity observations could be making muffins instead of a full cake. In such an example, since we are limited by oven size, we can parallelize low-fidelity experiments much easier than high fidelity ones.

We focus on multi-fidelity and batch methods that allow mimicking of sequentially choosing experiments and fidelities, this means we can select which experiments to run without worrying about selecting a batch size or limiting ourselves to single-fidelity batches!

5 Asynchronous Multi-fidelity Batch Optimization

5.1 Problem Setting

We now seek to formalize the problem setting. The method presented seeks to find the best possible solution, as *quickly* as possible. We are interested in:

$$x_* = \arg \max_{x \in \mathcal{X}} f(x)$$

Where \mathcal{X} denotes a *continuous* input space. We assume f is expensive to evaluate, but, we have access to lower fidelity approximations, $f^{(m)}$, which tend to be cheaper (for $m = 1, \dots, M$). These approximations may be biased or noisy.

Because we are trying to optimize with respect to time, we introduce a discrete time component. We denote the input of the i th experiment by $x_{i,t}^{(m)}$, where $t \in \{1, \dots, T\}$ denotes the time at which the experiment began, and $m \in \{1, \dots, M\}$ denotes the fidelity.

When we select an input point, $x_{i,t}^{(m)}$, we obtain a noisy observation of $f^{(m)}$. However, we may not observe it at time t . Instead, we observe it at time $t + \tau_i^{(m)}$, where $\tau_i^{(m)}$ can be a deterministic or random time. We denote the corresponding observation $y_{i,t+\tau_i}^{(m)}$. We assume the relationship between the observation and the experimental input is given by:

$$y_{i,t+\tau_i}^{(m)} = f^{(m)}(x_{i,t}^{(m)}) + \eta^{(m)}\epsilon_i, \quad (18)$$

where $\eta^{(m)}$ denotes the noise level. We assume ϵ_i is standard Gaussian, where the variance may depend on the fidelity level.

Finally we assume that each fidelity has an associated batch space $\lambda^{(m)}$ (which in practice typically increases with fidelity). We assume this batch space is not freed up until we have an observation. We also have a maximum budget which we cannot exceed at any one time, Λ . If we let λ_i denote the batch space associated with the i th observation, and

we let \mathcal{I} denote the index set of the unobserved queries, we can write this as the constraint:

$$\text{TotalBatchSpace}_t := \sum_{i \in \mathcal{I}} \lambda_i \leq \Lambda \quad (19)$$

This idea behind this constraint is that we may be able to run a lot of low-fidelity observations or a few high-fidelity observations or a mix of both. We note that this batch space is independent of the time it takes to query each fidelity. We are introducing this as to allow variable batch sizes. An example of this in practice, because coin cell batteries are smaller and use less material, we can concurrently run more experiments than for pouch cell experiments.

The **aim** of the algorithm would be to obtain the best possible approximation of the optimum point at time T .

5.2 A general algorithm for any acquisition function

A general algorithm can be constructed from all the tools mentioned above. For this we require: (a) A Multi-task Gaussian Processes model, because we will require information transfer between the fidelities, (b) A method that allows for asynchronous batching, and (c) A way of choosing which fidelity to query. We propose iteratively choosing the points, we first optimize a batch-modified acquisition function *on the target fidelity*:

$$x_{i+1,t} = \arg \max_{x \in \mathcal{X}} \tilde{\alpha}_t(x, M | D_t, \mathcal{Q}_t) \quad (20)$$

Where \mathcal{Q}_t is the batch of points being evaluated at time t , and $\tilde{\alpha}$ is a acquisition function modified to consider that we are currently evaluating \mathcal{Q}_t by either local penalizing or fantasizing. Once we have chosen the point, we can choose the fidelity. We consider two alternatives, the first one is the heuristic used on MF-GP-UCB:

$$m_{i+1,t} = \arg \min_{m \in \{0, \dots, M\}} \{m : \beta_t^{1/2} \sigma_t^{(m)}(x_{i+1,t}) > \gamma^{(m)} \text{ or } m = M\} \quad (21)$$

In other words, we query at the lower fidelities until the uncertainty at each fidelity is lower than some threshold $\gamma^{(m)} / \beta_t^{1/2}$. The second alternative is to consider the information-based criterion introduced by MF-MES:

$$m_{t+1} = \arg \max_{m \in \{0, \dots, M\}} \frac{\mathbb{E}_{f_{\mathcal{Q}} | D_t} [I(x, f^{(m)}(x_{i+1,t}); f_* | D_t, f_{\mathcal{Q}}, \mathcal{Q}_t)]}{\mathbb{E} [\tau^{(m)}]} \quad (22)$$

The main advantage of doing this, instead of optimizing MF-MES directly, is that we do not need to rely on approximating an information-based acquisition function during the optimization, and instead we only evaluate the expensive acquisition function M -times. In addition, it allows us to use specialist acquisition functions, as we shall see in the experiment section. As any acquisition function can be selected (including multi-objective acquisition functions), future work can extend the proposed methodology to cases with multiple objectives, which arise in many engineering applications [Park et al., 2018, Schweidtmann et al., 2018, Thebelt et al., 2022b, Badejo and Ierapetritou, 2022, Tu et al., 2022].

We then repeat this procedure until the maximum budget is used up. Then, at each time point, we check if there are any new observations. If there are, we update the model, and carry out the previous procedure until the budget is full again. The full procedure is detailed in Algorithm 1.

5.3 Parameter Estimation

In this section we provide brief and heuristic guidance for the estimation of parameters. In particular, all Gaussian Process models have learnable hyper-parameters. In addition, if we use equation (21) for fidelity-selection, then we introduce hyper-parameters relating to the fidelity thresholds, β_t and $\gamma^{(m)}$. For Local Penalization, we are also required to estimate the Lipschitz constant and the maximum value of the function. For Fantasizing we need to choose the number of fantasies we want. MES-based fidelity selection are parameter-free, but more computationally costly. For ease of notation, we write x_i to refer to $x_{i,t}^{(m)}$.

5.3.1 The kernel and noise parameters

We estimate the parameters of the GP, θ , by maximizing the marginal log likelihood [Rasmussen and Williams, 2005]:

$$\log p(y|x, \theta) = -\frac{1}{2} \log |K_{\theta}| - \frac{1}{2}(y - \mu)^T K_{\theta}^{-1}(y - \mu) - \frac{N}{2} \log(2\pi) \quad (23)$$

Algorithm 1 Asynchronous Multi-fidelity Batch Optimization

INPUT: Maximum Budget: Λ . Batch Spaces: $\lambda^{(m)}$; $m = 1, \dots, M$. Acquisition Function: α . Choice of Asynchronous Bayesian Optimization: Fantasies or Local Penalization. Choice of fidelity-selector: UCB or Information-based. [Optional] Fidelity Thresholds Parameters: $\gamma^{(m)}$; $m = 1, \dots, M$ and β_t . Number of Fantasies: S .

Begin algorithm:

```

for  $t = 1, 2, 3, \dots, T$  do
  Obtain observations  $\mathcal{Y}_t$  from queries  $\mathcal{X}_t$ , with index set  $\mathcal{I}_t$ 
   $\mathcal{Q}_t = \mathcal{Q}_{t-1} \setminus \mathcal{X}_t$  # remove observations from batch
   $D_t = D_{t-1} \cup (\mathcal{X}_t \times \mathcal{Y}_t)$  # expand data set
   $\text{TotalBatchSpace}_t = \text{TotalBatchSpace}_{t-1} - \sum_{j \in \mathcal{I}_t} \lambda^{m_j}$  # free up cost of evaluations
  Update Surrogate Model
  while  $\text{TotalBatchSpace}_t < \Lambda$  do
    if BBO Method is Local Penalization then
      Estimate Maximum Value,  $P$ , and Lipschitz Constant,  $L$ 
      Build Initial Acquisition Function  $\alpha_t(x, M|D_t)$ 
       $\hat{\alpha}_t(x, M|D_t) = \alpha_t(x, M|D_t) \prod_{x_q \in \mathcal{Q}} \psi(x_q; \hat{L}, \hat{P})$ 
    else if BBO Method is Fantasies then
       $\mathcal{S} \leftarrow \text{Sample } f_{\mathcal{Q}}|D_t \text{ (}S\text{ times)}$ 
       $\tilde{\alpha}_t(x, M|D_t) = \sum_{i=1}^S \alpha_t(x, M|D_t, \mathcal{S}_i, \mathcal{Q})$ 
    else if BBO Method is Thompson Sampling then
       $f_{\text{sample}} \sim \mathcal{GP}(\mu_t, \kappa_t|D_t)$ 
       $x_{t+1} = \arg \max_{x \in \mathcal{X}} f_{\text{sample}}(x)$ 
    end if
     $x_{i,t} = \arg \max \alpha_t(x, M|D_t)$ 
     $m_{i,t} = \text{FidelitySelector}(x_{i,t+1}, D_t, \mathcal{Q})$ 
     $\mathcal{Q}_t = \mathcal{Q}_t \cup \{x_{i,t}\}$ 
     $\text{TotalBatchSpace}_t = \text{TotalBatchSpace}_t + \lambda^{(m_{i,t})}$ 
     $i = i + 1$ 
  end while
end for

```

Where K_θ is the covariance matrix of the training set, and μ is the predictive mean on the training set. However, we must note that only the lowest fidelity will have observations across the whole search space. The higher fidelities will only get observations in promising areas, meaning that estimating the hyper-parameters directly may lead to inaccuracies. To counter this, we only train fully train the GP hyper-parameters on the lowest fidelity for any multi-fidelity methods. For the other fidelities, we fix the prior mean constant and the length-scales, and we only train the scaling constants and the likelihood noise.

5.3.2 Choosing the fidelity thresholds, $\gamma^{(m)}$

Recall that we use the fidelity thresholds to decide in which fidelity to experiment at, and therefore it is very important that they are tuned correctly. If they are too high, we will not use the lower fidelities effectively, but if they are too low we will be stuck in the lower fidelities for a long time. To counter this, Kandasamy et al. [2016a] proposes the following heuristic: initialise the thresholds as small values, and if the process does not experiment above the m th fidelity for more than $\tau^{(m+1)} / \tau^{(m)}$ time points, double the value of $\gamma^{(m)}$. If the time intervals are random, we can use expectations instead.

Alternatively, we found good experimental results were achieved by setting $\gamma = 0.1$. However, we note that all benchmarks were quasi-normalized beforehand so that the output values would be close to 1. In practice fixed thresholds should be carefully scaled with the outputs.

5.3.3 The penalization parameters

The local penalisers depend on two parameters, the Lipschitz constant, L , and the maximum value of the function, $P = f(x_*)$. In practice, we will never know them, so it is important to have a good method of estimating them. González et al. [2016] propose ways of estimating both.

Method	Reference	Multi-fidelity	Batching	Model
UCB	Srinivas et al. [2010]	✗	✗	Single GP
MF-GP-UCB	Kandasamy et al. [2016a]	Variance-based	✗	Independent GPs
MF-GP-UCB w LP	This work	Variance-based	Local Penalization	Independent GPs
PLAyBOOK (UCB)	Alvi et al. [2019]	✗	Local Penalization	Single GP
UCB-V-LP	This work	Variance-based	Local Penalization	MOGP
UCB-I-LP	This work	Information-based	Local Penalization	MOGP
TuRBO-TS	Eriksson et al. [2019]	✗	Thompson Sampling	Single GP
TuRBO-V-TS	This work	Variance-based	Thompson Sampling	MOGP
TuRBO-I-TS	This work	Information-based	Thompson Sampling	MOGP
MF-MES	Takeno et al. [2020]	Information-based	Fantasies	MOGP

Table 1: Summary of all the methods compared in this section. We split the table into three sections: the first one refers to UCB-based methods, the second to the our modifications of TuRBO, and for the third we include MF-MES as a general baseline. Variance-based and Information-based multi-fidelity refers to using Equations (21) and (22) (respectively) to choose which fidelity to query. Local penalization is implemented as described in [Alvi et al., 2019], using hard local penalizers and a local estimate of the Lipschitz constant. Thompson Sampling is carried out across a fixed grid in TuRBO trust regions. In all cases, for TuRBO, we use a single trust region. For all non-batching methods, we fill the batch through random sampling as to avoid idle resources. We used GPyTorch and BoTorch to implement the methods [Paszke et al., 2019, Gardner et al., 2018, Balandat et al., 2020].

The maximum value can be estimated cheaply with $\hat{P} = \max_i \{y_i\}$, or with the slightly less rough estimate $\hat{P} = \max_{x \in \mathcal{X}} \mu_t(x)$. We tend to prefer the first option, as it is slightly cheaper, and we expect the estimates to be very similar. To adapt it to the multi-fidelity case, we get an estimate independently for each fidelity, keeping in mind we are trying to mimic the sequential case.

Estimating the Lipschitz constant is slightly more elaborate. It can be shown that $L_\nabla = \max_{x \in \mathcal{X}} \|\nabla f(x)\|$ is a valid Lipschitz constant. In addition, we know the distribution of the gradient:

$$\nabla f(x) | D_t \sim \mathcal{N}(\mu_\nabla(x), \Sigma_\nabla^2(x))$$

where the mean vector is:

$$\mu_\nabla(x) = \partial K_{t,*}(x) \tilde{K}_t^{-1} y$$

For $\tilde{K}_t = K_t + \eta^2 I$ and $(\partial K_{t,*})_{i,l} = \partial k_t(x) / \partial x^{(i)}$, and y is the vector containing all observations so far. We can then estimate the Lipschitz constant as $\hat{L} = \max_{x \in \mathcal{X}} \|\mu_\nabla(x)\|$.

This could further be improved, Alvi et al. [2019] propose using the local estimator, $L_{\nabla,i} = \max_{x \in \mathcal{X}_i} \|\mu_\nabla(x)\|$, where \mathcal{X}_i is a local region around the input of the i th experiment. This allows the penalization to adapt to the smoothness of the area it is being evaluated in.

6 Experimental Results

6.1 Synthetic Benchmarks

We focus on implementing the same benchmarks as Kandasamy et al. [2016a]. We compare against a simple single-query, single-fidelity UCB [Srinivas et al., 2010], against single-query MF-GP-UCB [Kandasamy et al., 2016a], and against a single-fidelity PLAyBOOK [Alvi et al., 2019]. In the interest of giving a fairer comparison, all single-query methods are turned into batch methods by selecting the first query using the acquisition function, and then filling the rest of the batch with random queries. The results can be see in Figure 4, with the evaluation times for each fidelity shown in the title. We carry out the optimization until there is enough budget to get 200 high fidelity observations. For all experiments we set the batch size to 4, and assume that the batch space of the low and high fidelities is the same.

6.2 High-dimensional Optimization

To highlight the usefulness of our proposed method, we show how we can use a specialist function to do high-dimensional multi-fidelity Bayesian Optimization. BO traditionally struggles in high-dimensions where the size of the search spaces means the exploratory phase of classical algorithms is given too much importance. Eriksson et al. [2019]

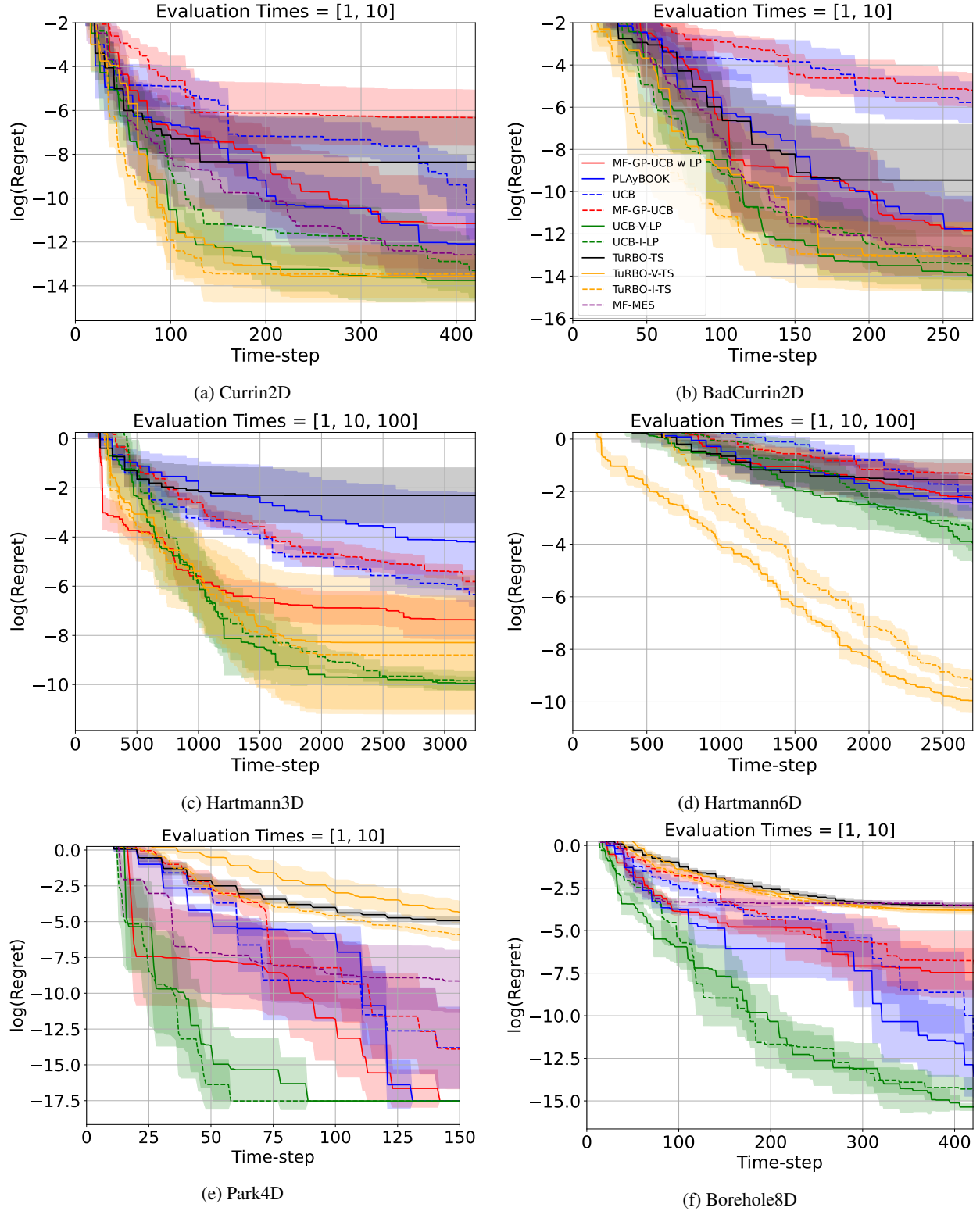


Figure 4: Results of synthetic experiments. We see that simply using UCB with our algorithm consistently achieves good results, always being one of the top performers. TuRBO also tends to perform fairly well, especially strongly in Hartmann6D, however, it also struggles badly in some benchmarks (Park4D and Borehole8D). MF-MES is not present in the Hartmann experiments due to the computational expense of testing the function when there are three fidelities.

proposed TuRBO which focuses on Local Optimization and tends to perform very well in high-dimensional settings. TuRBO uses a *trust region* approach which tries to avoid overconfidence in the surrogate model: trust region approaches often work well on high-dimensional chemical engineering applications Bajaj et al. [2018], Kazi et al. [2021, 2022]. We show, using the Ackley 40D benchmark, that we can use this acquisition function in our algorithm to obtain much better performance than other benchmarks. For this case we set the batch size to 20, and again assume that the batch space of low and high fidelities is the same. We set the budget as to allow 500 high-fidelity observations. The results are shown in Figure 5.

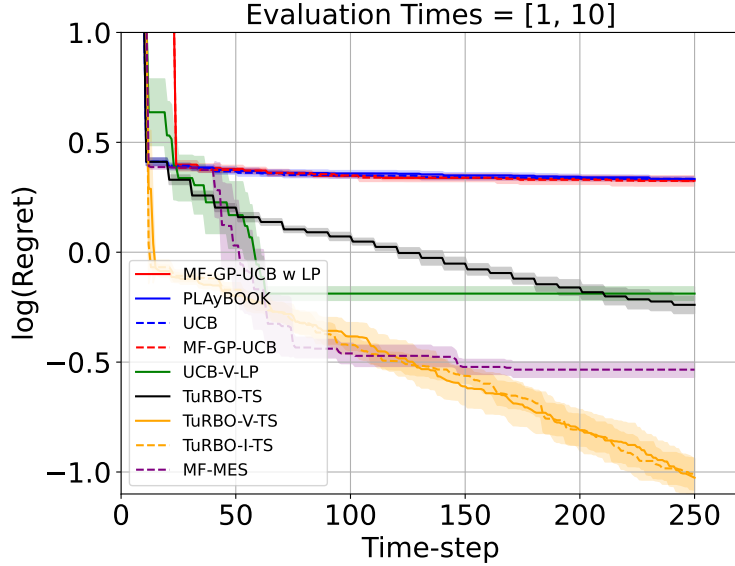


Figure 5: Results on Ackley 40D function. We can see that TuRBO is constantly improving, and outperforms other functions considerably. MF-MES and UCB-V-LP have good initial performance but begin to struggle after due to the over-exploration of classical BO.

6.3 Battery Material Design

We explore the application to the automatic design of battery materials. In this particular example, we aim to learn the best ratios of dopants in high-nickel cathode materials such that the specific capacity (electrochemically accessible charge per unit mass) is maximized. Our target is to find materials that have a high capacity over many charge-discharge cycles in pouch cell batteries. However, designing, building and testing such batteries requires many resources and long experimental cycles that take multiple months to process. As such, it is common for experiments to be carried out in parallel, where the batch size ranges between 10 and 20 concurrent queries, or experiments.

It is possible to obtain an approximation of pouch cell performance by considering coin cell batteries, where the materials are put into much smaller cylindrical containers requiring less material. In addition, we can reduce the duration of the experimental tests, perhaps by increasing the cycling rates or performing fewer charge-discharge cycles in total. Combining coin cell tests with accelerated test procedures allows us to get data in only a few weeks, and to carry out more experiments due to the lower material costs – however some of the real problem’s mechanisms may be suppressed. This represents the lower fidelity that we are interested in using.

For this example, we will be using an anonymized real-world data-set provided by BASF SE (the dataset, alongside the code used in the experiment section, can be found at <https://github.com/jpfolch/MFBoom>). We fit a Gaussian Process model to the data and using the method described in Wilson et al. [2020], we take a single sample to create our objective, $\tilde{f}^{(0)}$. We also took a second sample, $\tilde{f}^{(1)}$, to create the lower fidelity, meaning the function that we query is defined as:

$$f^{(m)}(x) = \begin{cases} \tilde{f}^{(0)}(x) & \text{if } m = 0 \\ \tilde{f}^{(1)}(x) & \text{if } m = 1 \end{cases} \quad (24)$$

Real battery materials laboratories vary in the degree of automation and the achievable experimental throughput. Here we assume we have a maximum batch budget of 20 and consider differing batch spaces. We assume that for each coin cell battery, or low fidelity, querying costs 1 unit, while the pouch cell battery, or high fidelity, costs 2 units. This means

we can concurrently do 20 coin cell experiments, or 10 pouch cell experiments, or a mix in between. We further assume that pouch cell experiments take 10 times longer than coin cell experiments, and set the time-budget to 300 (equivalent to being able to carry out 300 high-fidelity experiments). This is due to the combination of an accelerated test procedure with coin cell testing rather than an inherent speed-up associated with coin cells. The results are shown on Figure 6. We can see that the benefit to using the lower-fidelity with batching are substantial, as both methods that use both batching and multi-fidelity are significantly outperforming simple baselines, single-fidelity methods, and non-batching counterparts. For this specific example, we notice that using independent Gaussian Processes works surprisingly well. We did not compare against MF-MES or TuRBO due to complications in optimizing the acquisition function under the input constraints of the problem (see Appendix).

We further include a histogram, that shows how often we queried the low fidelity against the high fidelity. We compare UCB-V-LP (variance-based fidelity choice) against UCB-I-LP (information-based fidelity choice). The comparison can be seen in Figure 7.

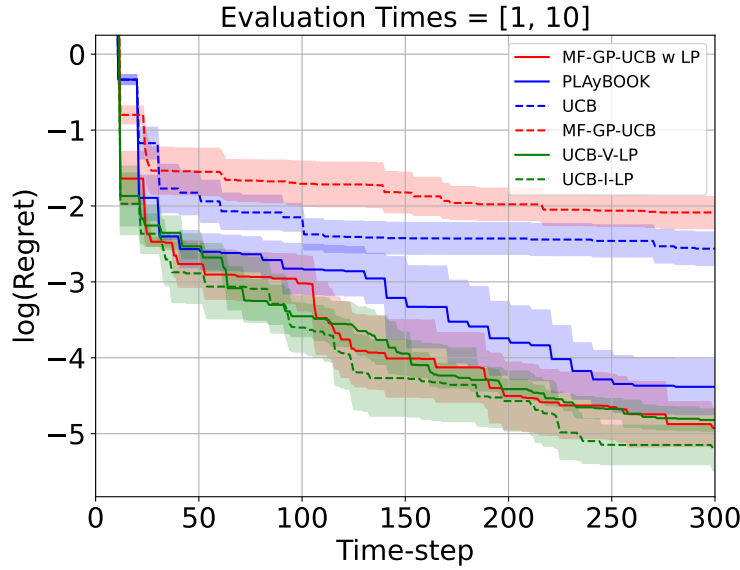


Figure 6: Results on battery design experiment. We can see that the asynchronous batching and multi-fidelity methods are significantly outperforming simple baselines (UCB), multi-fidelity without batching (MF-GP-UCB), and single-fidelity methods (PLAyBOOK). The performance of all batching multi-fidelity methods is similarly strong.

7 Conclusion and Discussion

In this paper we have explored methods in multi-fidelity and batch Bayesian Optimization, explaining why there is a close link between them and providing a comprehensive overview of the current state-of-the-art methods. We further show how we can leverage recent advances and propose an algorithm that allows practitioners to use acquisition functions well suited for their particular problem. We then empirically show the benefits of using such methods, illustrating their usefulness in both synthetic benchmarks, and real-life inspired problems.

Acknowledgments & Disclosure of Funding

JPF is funded by EPSRC through the Modern Statistics and Statistical Machine Learning (StatML) CDT (grant no. EP/S023151/1) and by BASF SE, Ludwigshafen am Rhein. The research was funded by Engineering & Physical Sciences Research Council (EPSRC) Fellowships to RM and CT (grant no. EP/P016871/1 and EP/T001577/1). CT also acknowledges support from an Imperial College Research Fellowship.

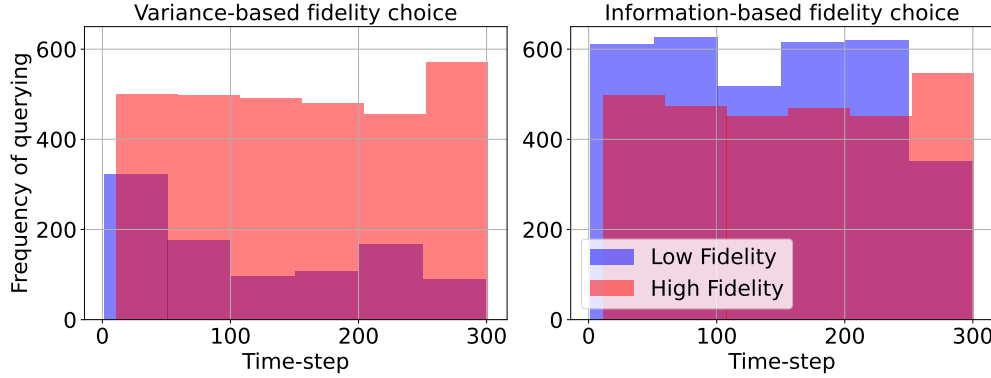


Figure 7: Experimental querying frequency comparison. The histogram above shows how often we queried the low and high fidelities for different time-intervals. We compare the querying frequency for the methods using UCB and Local Penalization, with different ways of choosing the fidelity – variance-based (left) against information-based (right). In both cases, we can see that towards the end of the optimization, there is decrease in low-fidelity querying, and an increase in high fidelity querying. However, information-based fidelity choice queries far more at the lowest fidelity – and seems to get marginally better results. This highlights the advantage of the information-based method being parameter-free, as the variance-based requires better tuning of the UCB thresholds to use the lower-fidelity at its full capacity.

References

Shuru Chen, Chaojiang Niu, Hongkyung Lee, Qiuyan Li, Lu Yu, Wu Xu, Ji-Guang Zhang, Eric J. Dufek, M. Stanley Whittingham, Shirley Meng, Jie Xiao, and Jun Liu. Critical Parameters for Evaluating Coin Cells and Pouch Cells of Rechargeable Li-Metal Batteries. *Joule*, 3(4):1094–1105, 2019.

Susanne Dörfler, Holger Althues, Paul Härtel, Thomas Abendroth, Benjamin Schumm, and Stefan Kaskel. Challenges and Key Parameters of Lithium-Sulfur Batteries on Pouch Cell Level. *Joule*, 4(3):539–554, 2020.

Ya-Tao Liu, Sheng Liu, Guo-Ran Li, and Xue-Ping Gao. Strategy of enhancing the volumetric energy density for lithium–sulfur batteries. *Advanced Materials*, 33(8):2003955, 2021.

Peter M Attia, Aditya Grover, Norman Jin, Kristen A Severson, Todor M Markov, Yang-Hung Liao, Michael H Chen, Bryan Cheong, Nicholas Perkins, Zi Yang, et al. Closed-loop optimization of fast-charging protocols for batteries with machine learning. *Nature*, 578(7795):397–402, 2020.

SP Asprey and S Macchietto. Statistical tools for optimal dynamic model building. *Computers & Chemical Engineering*, 24(2-7):1261–1267, 2000.

George EP Box and HL Lucas. Design of experiments in non-linear situations. *Biometrika*, 46(1/2):77–90, 1959.

Conor Waldron, Arun Pankajakshan, Marco Quaglio, Enhong Cao, Federico Galvanin, and Asterios Gavriilidis. An autonomous microreactor platform for the rapid identification of kinetic models. *Reaction Chemistry & Engineering*, 4:1623–1636, 2019.

William G Hunter and Albey M Reiner. Designs for discriminating between two rival models. *Technometrics*, 7(3): 307–323, 1965.

Calvin Tsay, Richard C. Pattison, Michael Baldea, Ben Weinstein, Steven J. Hodson, and Robert D. Johnson. A superstructure-based design of experiments framework for simultaneous domain-restricted model identification and parameter estimation. *Computers & Chemical Engineering*, 107:408–426, 2017.

Benjamin T Vincent. Hierarchical Bayesian estimation and hypothesis testing for delay discounting tasks. *Behavior Research Methods*, 48(4):1608–1620, 2016.

Adam Foster, Desi R Ivanova, Ilyas Malik, and Tom Rainforth. Deep Adaptive Design: Amortizing Sequential Bayesian Experimental Design. In *International Conference on Machine Learning*, pages 3384–3395, 2021.

Gaia Franceschini and Sandro Macchietto. Model-based design of experiments for parameter precision: State of the art. *Chemical Engineering Science*, 63(19):4846–4872, 2008.

Jialu Wang and Alexander W Dowling. Pyomo.DOE: An open-source package for model-based design of experiments in Python. *AIChE Journal*, page e17813, 2022a.

Ishan Bajaj, Akhil Arora, and M. M. Faruque Hasan. *Black-Box Optimization: Methods and Applications*, pages 35–65. Springer International Publishing, 2021.

Donald R Jones, Matthias Schonlau, and William J Welch. Efficient global optimization of expensive black-box functions. *Journal of Global Optimization*, 13(4):455–492, 1998.

Bobak Shahriari, Kevin Swersky, Ziyu Wang, Ryan P. Adams, and Nando de Freitas. Taking the Human Out of the Loop: A Review of Bayesian Optimization. *Proceedings of the IEEE*, 104(1):148–175, 2016.

Atharv Bhosekar and Marianthi Ierapetritou. Advances in surrogate based modeling, feasibility analysis, and optimization: A review. *Computers & Chemical Engineering*, 108:250–267, 2018.

Alexander Thebelt, Johannes Wiebe, Jan Kronqvist, Calvin Tsay, and Ruth Misener. Maximizing information from chemical engineering data sets: Applications to machine learning. *Chemical Engineering Science*, 252:117469, 2022a.

Kirthevasan Kandasamy, Gautam Dasarathy, Junier B Oliva, Jeff Schneider, and Barnabás Póczos. Gaussian Process Bandit Optimisation with Multi-fidelity Evaluations. *Advances in Neural Information Processing Systems*, 29, 2016a.

Shion Takeno, Hitoshi Fukuoka, Yuhki Tsukada, Toshiyuki Koyama, Motoki Shiga, Ichiro Takeuchi, and Masayuki Karasuyama. Multi-fidelity Bayesian optimization with max-value entropy search and its parallelization. In *International Conference on Machine Learning*, pages 9334–9345. PMLR, 2020.

Javier González, Zhenwen Dai, Philipp Hennig, and Neil Lawrence. Batch Bayesian Optimization via Local Penalization. In *Proceedings of the 19th International Conference on Artificial Intelligence and Statistics*, pages 648–657, 09–11 May 2016.

Ahsan Alvi, Binxin Ru, Jan-Peter Calliess, Stephen Roberts, and Michael A. Osborne. Asynchronous Batch Bayesian Optimisation with Improved Local Penalisation. In *International Conference on Machine Learning*, pages 253–262, 09–15 Jun 2019.

Kirthevasan Kandasamy, Akshay Krishnamurthy, Jeff Schneider, and Barnabas Poczos. Parallelised Bayesian Optimisation via Thompson Sampling. In *Proceedings of the Twenty-First International Conference on Artificial Intelligence and Statistics*, pages 133–142, 2018.

Jasper Snoek, Hugo Larochelle, and Ryan P Adams. Practical Bayesian optimization of machine learning algorithms. *Advances in Neural Information Processing Systems*, 25, 2012.

James Bergstra, Rémi Bardenet, Yoshua Bengio, and Balázs Kégl. Algorithms for hyper-parameter optimization. *Advances in Neural Information Processing Systems*, 24, 2011.

Lisha Li, Kevin Jamieson, Giulia DeSalvo, Afshin Rostamizadeh, and Ameet Talwalkar. Hyperband: A novel bandit-based approach to hyperparameter optimization. *The Journal of Machine Learning Research*, 18(1):6765–6816, 2017.

Satyajith Amaran, Nikolaos V Sahinidis, Bikram Sharda, and Scott J Bury. Simulation optimization: a review of algorithms and applications. *Annals of Operations Research*, 240(1):351–380, 2016.

Ke Wang and Alexander W Dowling. Bayesian optimization for chemical products and functional materials. *Current Opinion in Chemical Engineering*, 36:100728, 2022b.

Jose Pablo Folch, Shiqiang Zhang, Robert M Lee, Behrang Shafei, David Walz, Calvin Tsay, Mark van der Wilk, and Ruth Misener. SnAKE: Bayesian Optimization with Pathwise Exploration. *arXiv preprint arXiv:2202.00060*, 2022.

Alexander Thebelt, Jan Kronqvist, Miten Mistry, Robert M Lee, Nathan Sudermann-Merx, and Ruth Misener. ENT-MOOT: a framework for optimization over ensemble tree models. *Computers & Chemical Engineering*, 151:107343, 2021.

Alexander Thebelt, Calvin Tsay, Robert M Lee, Nathan Sudermann-Merx, David Walz, Tom Tranter, and Ruth Misener. Multi-objective constrained optimization for energy applications via tree ensembles. *Applied Energy*, 306:118061, 2022b.

Alexander Thebelt, Calvin Tsay, Robert M Lee, Nathan Sudermann-Merx, David Walz, Behrang Shafei, and Ruth Misener. Tree ensemble kernels for Bayesian optimization with known constraints over mixed-feature spaces. *arXiv preprint arXiv:2207.00879*, 2022c.

Alison Cozad, Nikolaos V Sahinidis, and David C Miller. Learning surrogate models for simulation-based optimization. *AICHE Journal*, 60(6):2211–2227, 2014.

Fani Boukouvala and Christodoulos A Floudas. ARGONAUT: AlgoRithms for Global Optimization of coNstrAined grey-box compUTational problems. *Optimization Letters*, 11(5):895–913, 2017.

Simon Olofsson, Mohammad Mehrian, Roberto Calandra, Liesbet Geris, Marc Peter Deisenroth, and Ruth Misener. Bayesian multiobjective optimisation with mixed analytical and black-box functions: Application to tissue engineering. *IEEE Transactions on Biomedical Engineering*, 66(3):727–739, 2018.

Seongeon Park, Jonggeol Na, Minjun Kim, and Jong Min Lee. Multi-objective Bayesian optimization of chemical reactor design using computational fluid dynamics. *Computers & Chemical Engineering*, 119:25–37, 2018.

Joel A Paulson and Congwen Lu. COBALT: COnstrained Bayesian optimizAtion of computationally expensive grey-box models exploiting derivative information. *Computers & Chemical Engineering*, 160:107700, 2022.

Akshay Kudva, Farshud Sorourifar, and Joel A Paulson. Constrained robust Bayesian optimization of expensive noisy black-box functions with guaranteed regret bounds. *AIChE Journal*, page e17857, 2022.

M. C. Kennedy and A. O’Hagan. Predicting the Output from a Complex Computer Code When Fast Approximations Are Available. *Biometrika*, 87(1):1–13, 2000.

Loic Le Gratiet. Recursive Co-Kriging Model for Design of Computer Experiments with Multiple Levels of Fidelity with an Application to Hydrodynamic, 2013.

Kurt Cutajar, Mark Pullin, Andreas Damianou, Neil Lawrence, and Javier Gonzalez. Deep Gaussian Processes for Multi-fidelity Modeling, 2019.

Kirthevasan Kandasamy, Gautam Dasarathy, Jeff Schneider, and Barnabas Poczos. The Multi-fidelity Multi-armed Bandit, 2016b.

Rajat Sen, Kirthevasan Kandasamy, and Sanjay Shakkottai. Multi-Fidelity Black-Box Optimization with Hierarchical Partitions. In *International Conference on Machine Learning*, pages 4538–4547, 2018.

Andre G Journel and Charles J Huijbregts. Mining geostatistics. 1976.

Pierre Goovaerts et al. *Geostatistics for natural resources evaluation*. Oxford University Press on Demand, 1997.

Mauricio A Alvarez, Lorenzo Rosasco, Neil D Lawrence, et al. Kernels for vector-valued functions: A review. *Foundations and Trends® in Machine Learning*, 4(3):195–266, 2012.

Fuzhen Zhuang, Zhiyuan Qi, Keyu Duan, Dongbo Xi, Yongchun Zhu, Hengshu Zhu, Hui Xiong, and Qing He. A comprehensive survey on transfer learning. *Proceedings of the IEEE*, 109(1):43–76, 2021.

Sinno Jialin Pan and Qiang Yang. A survey on transfer learning. *IEEE Transactions on knowledge and data engineering*, 22(10):1345–1359, 2009.

Weijun Li, Sai Gu, Xiangping Zhang, and Tao Chen. Transfer learning for process fault diagnosis: Knowledge transfer from simulation to physical processes. *Computers & Chemical Engineering*, 139:106904, 2020.

Bowen Li and Srinivas Rangarajan. A conceptual study of transfer learning with linear models for data-driven property prediction. *Computers & Chemical Engineering*, 157:107599, 2022.

Runda Jia, Shulei Zhang, and Fengqi You. Transfer learning for end-product quality prediction of batch processes using domain-adaption joint-Y PLS. *Computers & Chemical Engineering*, 140:106943, 2020.

Alexander W Rogers, Fernando Vega-Ramon, Jiangtao Yan, Ehecatl A del Río-Chanona, Keju Jing, and Dongda Zhang. A transfer learning approach for predictive modeling of bioprocesses using small data. *Biotechnology and Bioengineering*, 119(2):411–422, 2022.

David Ginsbourger, Janis Janusevskis, and Rodolphe Le Riche. *Dealing with Asynchronicity in Parallel Gaussian Process based Global Optimization*. PhD thesis, Mines Saint-Etienne, 2011.

Abdulelah S Alshehri, Rafiqul Gani, and Fengqi You. Deep learning and knowledge-based methods for computer-aided molecular design—toward a unified approach: State-of-the-art and future directions. *Computers & Chemical Engineering*, 141:107005, 2020.

Connor W Coley. Defining and exploring chemical spaces. *Trends in Chemistry*, 3(2):133–145, 2021.

Connor W. Coley, Dale A. Thomas, Justin A. M. Lummiss, Jonathan N. Jaworski, Christopher P. Breen, Victor Schultz, Travis Hart, Joshua S. Fishman, Luke Rogers, Hanyu Gao, Robert W. Hicklin, Pieter P. Plehiers, Joshua Byington, John S. Piotti, William H. Green, A. John Hart, Timothy F. Jamison, and Klavs F. Jensen. A robotic platform for flow synthesis of organic compounds informed by ai planning. *Science*, 365(6453), 2019.

Shibo Li, Robert Kirby, and Shandian Zhe. Batch multi-fidelity Bayesian optimization with deep auto-regressive networks. *Advances in Neural Information Processing Systems*, 34, 2021.

Zi Wang and Stefanie Jegelka. Max-value entropy search for efficient optimization. In *International Conference on Machine Learning*, pages 3627–3635. PMLR, 2017.

Henry B Moss, David S Leslie, Javier Gonzalez, and Paul Rayson. GIBBON: General-purpose information-based Bayesian optimisation. *Journal of Machine Learning Research*, 22(235):1–49, 2021.

Gordon Hüllen, Jianyuan Zhai, Sun Hye Kim, Anshuman Sinha, Matthew J Realff, and Fani Boukouvala. Managing uncertainty in data-driven simulation-based optimization. *Computers & Chemical Engineering*, 136:106519, 2020.

Carl Edward Rasmussen and Christopher K. I. Williams. *Gaussian Processes for Machine Learning (Adaptive Computation and Machine Learning)*. The MIT Press, 2005.

Yee Whye Teh, Matthias Seeger, and Michael I Jordan. Semiparametric latent factor models. In *International Workshop on Artificial Intelligence and Statistics*, pages 333–340. PMLR, 2005.

Jay M Ver Hoef and Ronald Paul Barry. Constructing and fitting models for cokriging and multivariable spatial prediction. *Journal of Statistical Planning and Inference*, 69(2):275–294, 1998.

Dave Higdon. Space and space-time modeling using process convolutions. In *Quantitative methods for current environmental issues*, pages 37–56. Springer, 2002.

Mark van der Wilk, Carl Edward Rasmussen, and James Hensman. Convolutional Gaussian Processes. *Advances in Neural Information Processing Systems*, 30, 2017.

Andreas Damianou and Neil D Lawrence. Deep Gaussian processes. In *Artificial intelligence and statistics*, pages 207–215. PMLR, 2013.

David JC MacKay. A practical Bayesian framework for backpropagation networks. *Neural Computation*, 4(3):448–472, 1992.

Radford M Neal. *Bayesian learning for neural networks*, volume 118. Springer Science & Business Media, 2012.

Pavel Izmailov, Sharad Vikram, Matthew D Hoffman, and Andrew Gordon Gordon Wilson. What are Bayesian neural network posteriors really like? In *International Conference on Machine Learning*, pages 4629–4640, 2021.

Julien Villemonteix, Emmanuel Vazquez, and Eric Walter. An informational approach to the global optimization of expensive-to-evaluate functions. *Journal of Global Optimization*, 44(4):509–534, 2009.

Philipp Hennig and Christian J Schuler. Entropy Search for Information-Efficient Global Optimization. *Journal of Machine Learning Research*, 13(6), 2012.

José Miguel Hernández-Lobato, Matthew W Hoffman, and Zoubin Ghahramani. Predictive entropy search for efficient global optimization of black-box functions. *Advances in Neural Information Processing Systems*, 27, 2014.

Ben Tu, Axel Gandy, Nikolas Kantas, and Behrang Shafei. Joint entropy search for multi-objective Bayesian optimization. *arXiv preprint arXiv:2210.02905*, 2022.

Carl Hvarfner, Frank Hutter, and Luigi Nardi. Joint entropy search for maximally-informed Bayesian optimization. *arXiv preprint arXiv:2206.04771*, 2022.

Artur M Schweidtmann, Adam D Clayton, Nicholas Holmes, Eric Bradford, Richard A Bourne, and Alexei A Lapkin. Machine learning meets continuous flow chemistry: Automated optimization towards the Pareto front of multiple objectives. *Chemical Engineering Journal*, 352:277–282, 2018.

Oluwadare Badejo and Marianthi Ierapetritou. Integrating tactical planning, operational planning and scheduling using data-driven feasibility analysis. *Computers & Chemical Engineering*, 161:107759, 2022.

Niranjan Srinivas, Andreas Krause, Sham Kakade, and Matthias Seeger. Gaussian Process Optimization in the Bandit Setting: No Regret and Experimental Design. In *International Conference on Machine Learning*, pages 1015–1022, 2010.

David Eriksson, Michael Pearce, Jacob Gardner, Ryan D Turner, and Matthias Poloczek. Scalable global optimization via local Bayesian optimization. *Advances in Neural Information Processing Systems*, 32, 2019.

Adam Paszke, Sam Gross, Francisco Massa, Adam Lerer, James Bradbury, Gregory Chanan, Trevor Killeen, Zeming Lin, Natalia Gimelshein, Luca Antiga, Alban Desmaison, Andreas Kopf, Edward Yang, Zachary DeVito, Martin Raison, Alykhan Tejani, Sasank Chilamkurthy, Benoit Steiner, Lu Fang, Junjie Bai, and Soumith Chintala. PyTorch: An Imperative Style, High-Performance Deep Learning Library. In *Advances in Neural Information Processing Systems*, pages 8024–8035. Curran Associates, Inc., 2019.

Jacob R. Gardner, Geoff Pleiss, David Bindel, Kilian Q. Weinberger, and Andrew Gordon Wilson. Gpytorch: Blackbox matrix-matrix Gaussian Process inference with GPU acceleration. *Advances in Neural Information Processing Systems*, pages 7576–7586, 2018.

Maximilian Balandat, Brian Karrer, Daniel R. Jiang, Samuel Daulton, Benjamin Letham, Andrew Gordon Wilson, and Eytan Bakshy. BoTorch: A Framework for Efficient Monte-Carlo Bayesian Optimization. In *Advances in Neural Information Processing Systems*, 33, 2020.

Ishan Bajaj, Shachit S Iyer, and MM Faruque Hasan. A trust region-based two phase algorithm for constrained black-box and grey-box optimization with infeasible initial point. *Computers & Chemical Engineering*, 116:306–321, 2018.

Saif R Kazi, Michael Short, and Lorenz T Biegler. A trust region framework for heat exchanger network synthesis with detailed individual heat exchanger designs. *Computers & chemical engineering*, 153:107447, 2021.

Saif R Kazi, Ishanki A De Mel, and Michael Short. A new trust-region approach for optimization of multi-period heat exchanger networks with detailed shell-and-tube heat exchanger designs. In *Computer Aided Chemical Engineering*, volume 49, pages 241–246. Elsevier, 2022.

James Wilson, Viacheslav Borovitskiy, Alexander Terenin, Peter Mostowsky, and Marc Deisenroth. Efficiently Sampling Functions from Gaussian Process Posteriors. In *International Conference on Machine Learning*, pages 10292–10302, 13–18 Jul 2020.

Diederik Kingma and Jimmy Ba. Adam: A Method for Stochastic Optimization. *International Conference on Learning Representations*, 12 2014.

A Notation Table

General Notation

\mathcal{X}	Input space / Search space
f_*, x_*	Optimal function value, input at which the optimum is achieved
t	Time-index
$x_i^{(m)}$	Input to experiment, indexed by i , at fidelity m
T	Final time-step
M	Number of different fidelities
m	Fidelity index, must lie in $\{0, 1, \dots, M\}$
f	Latent function we want to optimize
D_t	Data-set at time t
η^2	Variance of observation noise
μ_0	Prior GP mean function
μ_t	Mean of posterior GP at time t
k_0	Prior GP co-variance function
$(k_t)^2$	Co-variance function of posterior GP at time t
$\tau_i^{(m)}$	Time-delay between querying the i th experiment (at fidelity m) and receiving an observation
$\lambda^{(m)}$	Batch space of an experiment at fidelity m
$\Lambda^{(m)}$	Maximum total batch space allowed
TotalBatchSpace $_t$	The total batch space of the unobserved queries at time t

Multi-fidelity Modelling

$f^{(m)}$	Latent function we used to approximate f at the m th fidelity
$\eta^{(m)}$	Noise level at the m -th fidelity
$D^{(m)}$	Data-set for the m -th fidelity
\mathcal{B}	Matrix of task-dependencies, learnt hyper-parameter of linear multi-task kernel
$k^{(I)}$	Kernel for measuring similarity among inputs
$k^{(F)}$	Kernel for measuring similarity among fidelities or tasks
W	Number of latent GPs assumed by the model
w	Index of latent GP

Bayesian Optimization

$\sigma_t(x)$	Posterior GP standard deviation at time t and input x
$\sigma_t^{(m)}(x)$	Posterior GP standard deviation at time t , input x and fidelity m
$\alpha(x)$	Acquisition function evaluated at input x
$\alpha^{(m)}(x)$	Upper-confidence bound generated using the m -th fidelity
$\zeta_{MAX}^{(m)}$	Maximum bias between fidelity m and the target fidelity
$\gamma^{(m)}$	Threshold used to decide if fidelity m should be queried
$I(\cdot, \cdot; \cdot)$	Information gain
$H(\cdot)$	Entropy
Q_t	Batch of points being evaluated at time t , but still unobserved
$\psi(x; x_j)$	Penalizing function centered at x_j
L	Lipschitz constant of f
$B_\delta(x)$	Open ball of radius δ , centered at x

$x_{i,t}^{(m)}$	Input to the i th experiment; t denotes the time at which evaluation started and m the fidelity
$y_{i,t'}^{(m)}$	Output to the i th experiment; t' denotes the time at which evaluation finished and m the fidelity
$\epsilon^{(m)}$	Noise level for m th fidelity
$\lambda^{(m)}, \lambda_i$	Batch space of m th fidelity, Batch space of i th experiment
Λ	Maximum cumulative batch space

B Implementation Details

We include implementation details about the methods used and the benchmarks. For full details, we refer any reader to the code, available at <https://github.com/jpfolch/MFBoom>.

B.1 Gaussian Processes

To implement the Gaussian Processes, we used the GPyTorch [Gardner et al., 2018] and PyTorch Paszke et al. [2019] libraries. When using independent Gaussian Processes, we used an RBF kernel:

$$k_{RBF}(x_1, x_2) = \theta_0 \exp\left(-\frac{1}{2}(x_1 - x_2)^T \Theta^{-2}(x_1 - x_2)\right) \quad (25)$$

Where θ_0 is a scaling constant, and $\Theta = \text{diag}(\ell_1, \dots, \ell_d)$, where ℓ_i represents the length-scale of the i th dimension. For Multi-Task Gaussian Processes, we used the kernel:

$$K(x, x') = \sum_{w=1}^W k_w^{(I)}(x, x') \mathcal{B}_w$$

where each $k_w^{(I)}(x, x')$ is given by an RBF kernel, an in Equation (25), each with *different hyper-parameters*. This choice was made to allow the model to vary the hyper-parameters at each fidelity. We further set the hyper-parameters $W = 2M$ and $\text{rank}(\mathcal{B}_w) = M$, where M is the number of fidelities in the problem. This choice was arbitrary, but yielded good results. The kernel hyper-parameters whose value we don't explicitly mention were all learnt by maximizing the marginal log-likelihood [Rasmussen and Williams, 2005].

To initialize the hyper-parameters, we trained a Gaussian Process model on $80 \log(d)$ randomly sampled data-points, and maximized the marginal log-likelihood. The data-points were then discarded, and the hyper-parameters from the initial GP were used to initialize the hyper-parameters of the GP used by Bayesian Optimization methods. We then retrained the hyper-parameters every time we obtained twenty new observations of either fidelity. To optimize the marginal log-likelihood, we used ADAM [Kingma and Ba, 2014] across 75 epochs, with a learning rate of 0.1.

To avoid any ill-behaviour, we also put a Smoothed Box Prior on each hyper-parameter. For length-scales the box went from 0.025 to 0.6, for the output-scale from 0.05 to 2, for the noise from 10^{-5} to 0.2, and for the prior mean constant from -1 to 1. All these values were chosen based on the scaling of the objective functions.

B.2 Methods

All Bayesian Optimization methods were implemented using GPyTorch [Gardner et al., 2018] and BoTorch [Balandat et al., 2020]. For the synthetic benchmarks, the acquisition functions were optimized using ADAM [Kingma and Ba, 2014] with a learning rate of 0.01 for 75 epochs. The optimization procedure was first evaluated on 7500d (independent GP methods), 7500 (multi-task based methods), or 3750 (MF-MES), random inputs, and the gradient optimization was multi-started on the best 10 outputs. The differences in number of points evaluated is based on the computational burden of each method.

B.2.1 TuRBO

In contrast, TuRBO [Eriksson et al., 2019] was optimized by grid search inside the trust region, using a Sobol grid of size $\min(5000, \max(2000, 200d))$.

To grow, shrink or move the trust region, we *only considered the high-fidelity observations*.

B.3 MF-MES

We created our own implementation of MF-MES (see Takeno et al. [2020] for notation that follows). We generated 100 samples of $f_* := \max f(x)$ using Thompson Sampling on a Sobol grid of size 7500. We also used 100 fantasies of f_Q to approximate the integral when doing asynchronous Bayesian Optimization.

The numerical integration was done using the Trapezium Rule, with the integration range broken into 500 intervals. For the integration range, we used $[-10^k, 10^k]$, where k was chosen to be the smallest element from $\{-6, \dots, 2\}$, such that $\eta(10^k) < 10^{-30}$.

Whenever we would detect issues from singular matrices while calculating MF-MES, we added 10^{-30} to the diagonal to obtain numerically stable behaviour.

B.4 Benchmark Details

All benchmarks are considered in the hyper-cube $[0, 1]^d$, where d is the problem dimension.

B.4.1 Battery

For the battery example, we considered a combinatorial constraint and an equality constraint. The benchmark is 6-dimensional, but we assume only three dimensions are allowed to be active at every moment, i.e.:

$$x_i = x_j = x_k = 0 \quad \text{for } i \neq j \neq k \quad (26)$$

where $i, j, k \in \{1, 2, \dots, 6\}$. We further have the equality constraint:

$$x_{i_a} + x_{j_a} + x_{k_a} = 1 \quad (27)$$

where i_a, j_a, k_a represent the *active* problem dimensions. To optimize with these constraints, we create a 2-dimensional Sobol grid, and filter out all points such that $x_0 + x_1 > 1$. We then calculate $x_2 = 1 - x_1 - x_0$. Finally, we expand the grid to all 20 possible combinations of active variables.

Due to these constraints, we do not consider TuRBO (trust region and intersection of feasible region might be too small) or MF-MES (grid size is too large to optimize the acquisition function comfortably) on the Battery benchmark.